Wideband Circularly Polarized Metamaterial-based Antenna employing Metasurface Structure

Tabassum, Samia
Chittagong University of Engineering and Technology (CUET)

Shil, Anaynna
Chittagong University of Engineering and Technology (CUET)

Jahan, Nusrat
Chittagong University of Engineering and Technology (CUET)

https://doi.org/10.5109/4102461

出版情報：Proceedings of International Exchange and Innovation Conference on Engineering & Sciences (IEICES). 6, pp.40-45, 2020-10-22. Interdisciplinary Graduate School of Engineering Sciences, Kyushu University
バージョン：
権利関係：

Wideband Circularly Polarized Metamaterial-based Antenna employing Metasurface Structure

Samia Tabassum[1], Anaynna Shil[1], Nusrat Jahan[1]
[1]Chittagong University of Engineering and Technology (CUET)
Corresponding author email: u1502110@student.cuet.ac.bd

ABSTRACT*: In this work, a novel wideband compact and low-profile metamaterial-based antenna has been proposed. The introduction of metasurface layer between the patch and ground plane improves antenna's performance, considerably. Our proposed circularly polarized (CP) antenna has been realized by two pairs of radiators. The CP characteristics have been obtained by placing two radiators in X-polarized wave and two in Y-polarized wave. Each radiator is carefully designed with epsilon negative transmission line (ENG-TL) to generate zeroth-order resonance (ZOR). Our proposed antenna achieves a gain of 4.94 dBiC, which is almost 0.58 dBiC higher than the structure without metasurface. Also, the operating bandwidth and the simulated axial ratio bandwidth (ARBW) of our proposed antenna improves to 676.3 MHz and 474.1 MHz.*

Keywords: Metamaterial; Metasurface; Circularly polarized.

1. INTRODUCTION

The increasing demand of high data-rate wireless communication motivates us to design compact size antenna, which is a major component of wireless transceiver. Researchers and academia are putting lots of effort to improve the antenna performances to implement low loss and compact wireless systems.

To solve the issue of transmitter and receiver orientation in sensitivity, circularly polarized (CP) structures have been immensely used. Circularly polarized (CP) antenna occupies higher capabilities of mitigating polarization mismatch and suppressing multipath interferences. It is therefore more preferable to wireless communication systems, such as the global navigation satellite system (GNSS), satellite communication system and radio frequency identification (RFID) system [1]. A dual-wideband CP antenna [2] based on the strategy of combining multi-mode resonances was proposed. Here, the primary radiators were two barbed-shape dipoles and two bowtie dipoles printed on the same substrate. For the low-profile antenna design, wider bandwidth and axial ratio, the radiators were placed over an artificial magnetic conductor (AMC). But it has lower gain. A low-profile, wideband and high gain CP crossed dipole antenna [3] consisting of two stepped patch dipoles, a thin dielectric slab and an irregular ground plane is introduced. A single feed ultra-wideband circularly polarized antenna is proposed and to enhance the Front-to-Back Ratio (FBR), a novel composite cavity is deployed [4]. Park et. al. used zeroth-order resonance based omni-directional CP antenna to improve the axial ratio [5]. Coplanar waveguide fed dual band linear and circularly polarized antenna with composite split ring resonator has been designed to reduce size and improve gain [6]. Also, dual band circularly polarized antenna with small size has been designed by incorporating a trimmed square patch antenna and a (2×2) triangle mushroom antenna [7]. But the entire aforementioned antenna suffers from narrow bandwidth, narrow axial ratio bandwidth, poor gain, larger size and design complexity.

Metamaterials (MMs) are three-dimensional (3D) artificial composite nanostructures which have extraordinary properties. They are used for guiding and controlling the flow of electromagnetic waves. They possess various attractive novel optical effects and applications not attainable using natural materials [8]-[9]. Metamaterial structure realized by composite right-left handed (CRLH) has been extensively used for both size reduction and performance enhancement. The CRLH transmission line was realized to design compact zeroth-order resonating wideband antennas [10]. A metamaterial based CP antenna [11] employing ENG-TL has been designed to improve the gain with lesser size of single feed. In [12], new characteristics of operation of the multilayers such as the substrate of epsilon-near-zero (ENZ) materials are introduced. The presence of the ENZ substrate leads to the quickly changing and extreme values of module and phase of amplitude reflection coefficients. Cube-shaped unit cells [13] are designed. They construct 3-D quasi-isotropic metamaterials in the microwave region. By inserting additional inductance into the metallic mesh, effective permittivity of the composite structures is reduced.

A metamaterial surface also known as metasurface is a two-dimensional (2D) structure of a metamaterial with sub-wavelength thickness. Metasurfaces research is very significant because of the ability to manipulate electromagnetic waves in microwave and optical frequencies. They have many advantages such as having light weight, ease of fabrication and ability to control wave propagation both on the surface and in the surrounding free space [14]. The performance of the metasurfaces is controlled by the sizes and shapes of the unit cell of the metasurface that are fabricated on the dielectric substrate [15] which can be explained with the following equation:

$$n_{eff} = \eta_g(xn_{sub} + (1-x)n_{air}) \quad (1)$$

Here, n_{eff} is the effective refractive index, x is substrate weight factor, η_g is the geometrical factor, n_{sub} and n_{air} are refractive indices of substrate and air, respectively.η

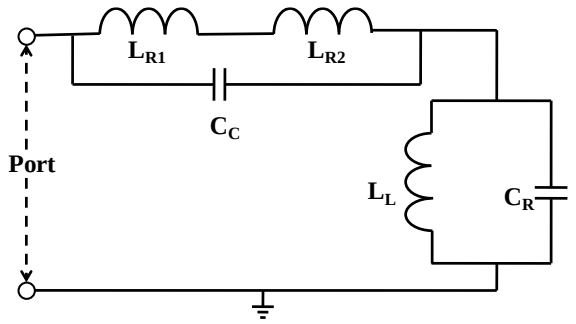

(a)

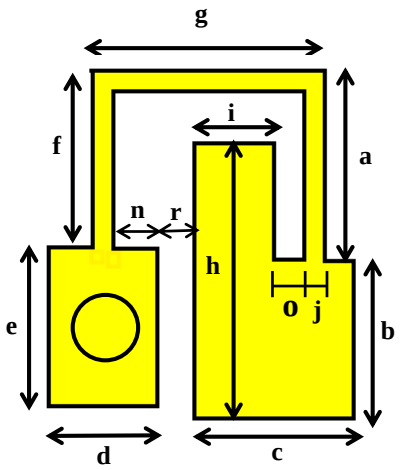

(b)

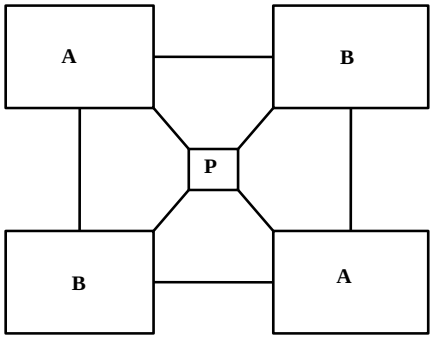

(c)

Fig. 1. (a) Equivalent circuit diagram of unit cell of patch. (b) Top view of unit cell of patch realization. (c) Block diagram of the proposed CP antenna.

Table 1. Optimized dimension of the proposed antenna unit cell

Parameter	Unit cell A (mm)	Unit cell B (mm)
a	3.65	3.65
b	2.75	3.75
c	3	2.8
d	2	2
e	3	3
f	3.4	4.15
g	4.4	4.15
h	5.25	6
i	1.5	1.25
j	0.4	0.4
n	0.8	0.8
o	0.55	0.55
r	0.75	0.75

can be varied with respect to the structures of the unit cell [16]. Metasurface structure can be easily fabricated due to their planar structure using planar fabrication tools [15]. Conversion from linear to circular polarization and bandwidth improvement of a conventional antenna are analyzed [17]. Here, the unit cell of the proposed polarization conversion metasurface (PCM) consists of square and L-shaped patches separated by an L-shaped slot printed on an FR4 substrate. Low-profile circularly polarized antenna based on fractal metasurface and fractal resonator has been designed to obtain high gain and wide axial ratio bandwidth [18]. Two microstrip patch antennas with single and multiple Octagonal Complementary Split Ring Resonator Structure (OCSRR) loaded on the ground plane was designed and fabricated [19]. In [20], the design has octagonal shape SRR structure. It specifies the stable and consistent E & H plane patterns with low cross polarization, acceptable gain, radiation efficiency and better impedance matching at operating wireless communication bands.

In this work, introduction of metasurface into the CP antenna results in an improved antenna gain. Also, a higher bandwidth and improved axial ratio are achieved. The electromagnetic (EM) simulations throughout the manuscripts has been done using Computer Simulation Technology (CST) design studio.

2. PROPOSED ANTENNA DESIGN

Our proposed CP antenna is comprised of four-unit cells interconnected to each other. The CP antenna is widely used because of its better flexibility towards the orientation of the transmitting and receiving antenna. It also minimizes the multipath effects including constructive and destructive interference and phase shifting of the signal. The equivalent circuit of the proposed antenna unit cell is shown in Fig. 1(a). The equivalent circuit is realized by using two rectangular patches and a spiral strip to connect the patches, as shown in Fig. 1(b) [11]. The series inductance L_{R1} is realized by the rectangular patch of area $h \times c$. The interconnected spiral strip of area $(a + g + f) \times j$ and rectangular patch of area $e \times d$ is contributing to the other series inductance L_{R2}. Coupling capacitor (C_C) is realized by the capacitive coupling between the patch and spiral strip. The shunt inductance (L_L) is realized by the shorted via between the smaller patch and ground plane. The shunt capacitor (C_R) is due to the capacitive coupling between the top radiator and ground plane. The orientation of the radiators is shown in Fig. 1(c), where cells A and B are interconnected with each other through a port (P), which possesses an area of $k \times m$.

For measurement of the proposed design, a coaxial cable is inserted in the top metal layer through the ground plane and positioned in port (P), which is pointed in Fig. 2(a). The total size of the antenna is $20\,mm \times 20\,mm \times 2.4\,m$. The position of the coaxial cable and vias is shown in Fig. 2(b). Here, Coaxial feeding technique is used. Coaxial feed point is at $(X, Y) = (1.5\text{ mm}, 1.5\text{ mm})$ with an inner and outer diameter of 1.4 mm and 5 mm. Each radiator contains a spiral strip and a shorted via. To design this antenna, substrate of FR-4 (lossy) type material is chosen with a given dielectric constant (ε_r) and loss tangent (δ).

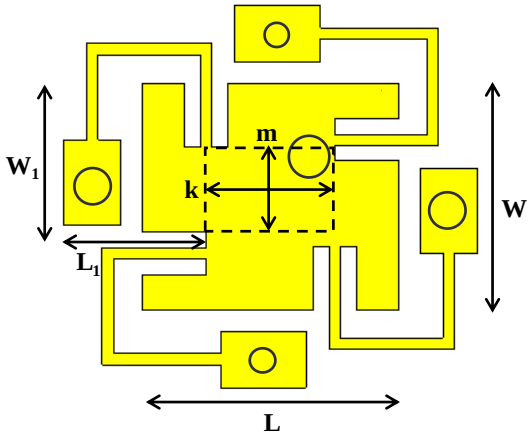

(a)

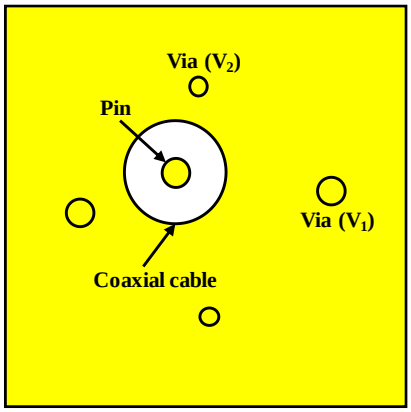

(b)

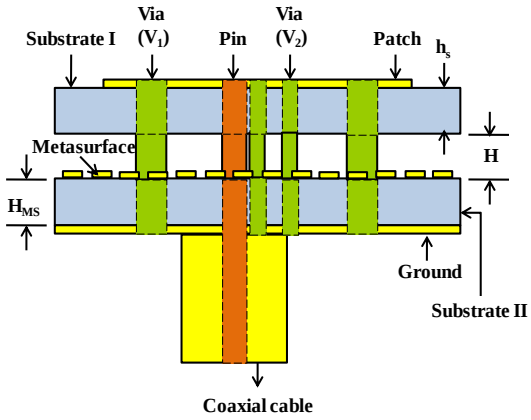

(c)

Fig. 2. (a) Front view (b) Back view & (c) Side view of the proposed antenna.

Dimensions of optimized parameters of the proposed antenna are given in Table 1 and Table 2, respectively.

Metamaterial based CP antenna is suitable for the design of miniaturized low-profile antenna. We choose epsilon negative (ENG) metamaterial which uses spiral strips for obtaining negative value of epsilon [21]. These metal spiral strip exhibit high-pass behavior for an incoming plane wave, whose electric field is parallel to the spiral strip [21]. For bandwidth and gain enhancement, a metasurface is employed between the top and bottom metal layers. A metasurface has the advantages of being ultrathin, low cost and ultralight. A finite sized metasurface structure yield extra resonances for the radiation structure [22], propagation of surface waves on the metasurface contribute to this extra

Table 2. Optimized dimension of the proposed antenna

Parameter	Value (mm)
h_s	0.08
H_{MS}	0.08
H	0.08
W	8
L	9
W_1	6.63
L_1	5
k	4.5
m	3
ε_r	4.3
δ	0.025
V_1	0.6
V_2	0.4

resonance frequency. The propagating constant (β_{SW}) of the surface waves travelling and decaying away from the metasurface is related to the decay constant (α) and the frequency (ω) by the expression of equation (2).

$$\beta_{SW} = \frac{\pi}{N \times P}$$
$$\beta_{SW} = \sqrt{\eta^{\,2}\omega^2 + \alpha^2} \quad (2)$$

Here, β_{SW} = Propagation constant of the surface wave resonances
N = The number of cells
P = Periodicity of the metasurface
η = Intrinsic impedance
ω = Frequency
α= Decay constant

The heights of substrate I and II are h_s and H_{MS}, as

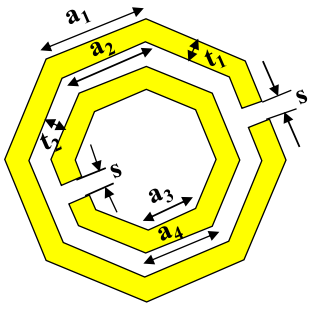

(a)

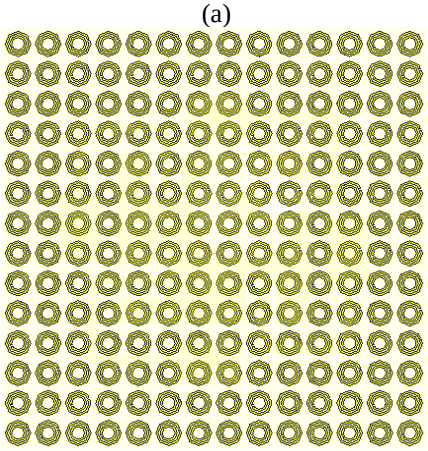

(b)

Fig. 3. (a) Geometric configuration of metasurface unit cell. (b)Top view of metasurface with (14×14) unit cells.

Table 3. Optimized dimension metasurface layer unit cell

Parameter	Value (mm)
a_1	0.46
a_2	0.38
a_3	0.23
a_4	0.31
t_1	0.1
t_2	0.1
s	0.08

shown in Fig. 2(c). The height H represents the air gap between two substrates. Octagonal split resonant ring (SRR) [23] is used as unit cell which is based on the C shape SRR shows in Fig. 3(a). Bandwidth enhancement is achieved with the proposed antenna having multiple octagonal split resonant ring structures. The metasurface layer is shown in Fig. 3(b), where octagonal periodic structures are realized in between the top and bottom metal layer. The metasurface consists of (14×14) unit cells, which are printed periodically on substrate II. Copper is chosen for patch, ground and metasurface material. Dimensions of optimized parameters for metasurface unit cell are given in Table 3.

There are two types of polarized waves- (i) X-polarized waves and (ii) Y-polarized waves. Unit cell A and B generate the X and Y-polarized waves respectively and this eventually contributes to the CP waves. CP can be controlled by controlling the radius of shorted vias (V_1) and (V_2).

3. SIMULATED RESULTS

The simulated scattered (|S|) parameter (S_{11}) and ARBW (Axial ratio bandwidth) of our proposed antenna are shown in Fig. 4 and Fig. 5, respectively. The calculated bandwidth (BW) of the antenna is 676.3 MHz $(6.458 - 7.1343)$ GHz. The calculated fractional bandwidth (FBW) is 9.95%, which can be calculated as (3).

$$FBW = \frac{f_{max} - f_{min}}{f_C} \times 100\% = \frac{BW}{f_C} \quad (3)$$

Where, f_C is the centre frequency of the antenna. The FBW of our proposed antenna improves by 1.04 times compared to [11]. The simulated axial ratio bandwidth (ARBW) is 474.1 MHz, which is improved by 344.1

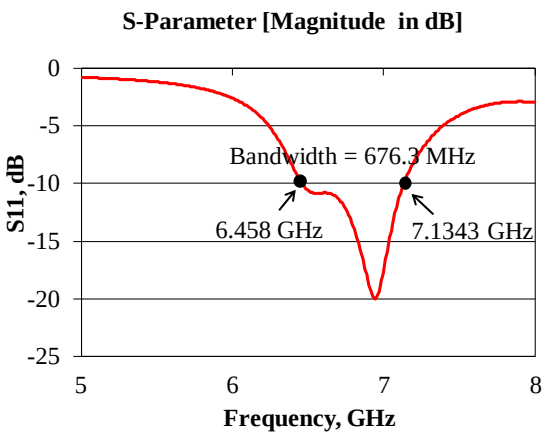

Fig. 4. Simulated scattered parameter ($|S_{11}|$) of the proposed antenna.

MHz in comparison to the work in [11]. The calculated gain is plotted in Fig. 6, where we can conclude that the introduction of the metasurface structure improves the antenna gain to 4.94 dBic at 6.85 GHz.

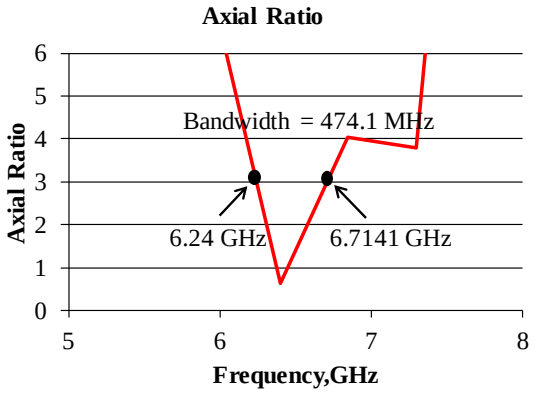

Fig. 5. Simulated ARBW of the proposed antenna.

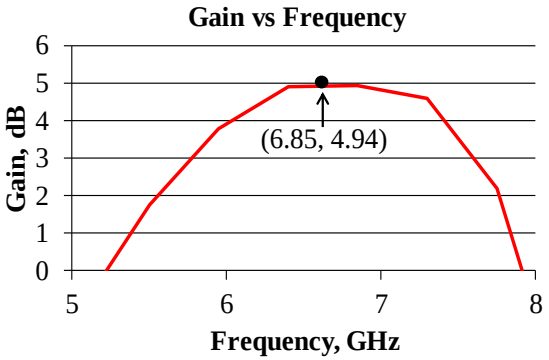

Fig. 6. Simulated gain of the proposed antenna.

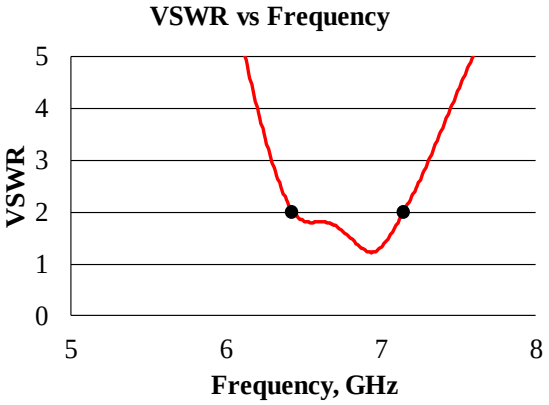

Fig. 7. VSWR vs Frequency curve.

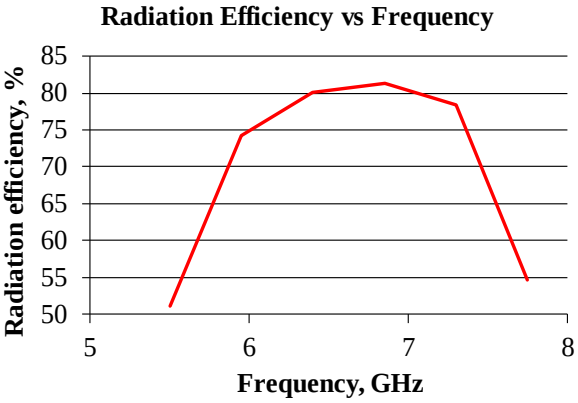

Fig. 8. Simulated radiation efficiency of the proposed antenna.

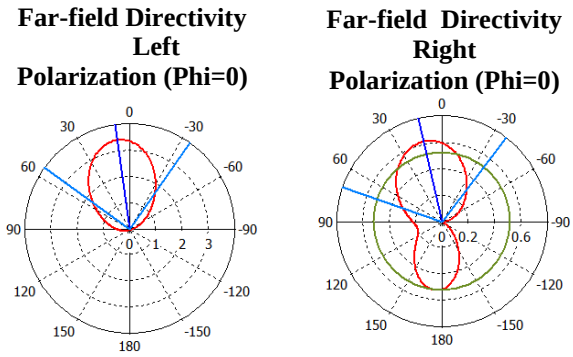

(a) XZ plane

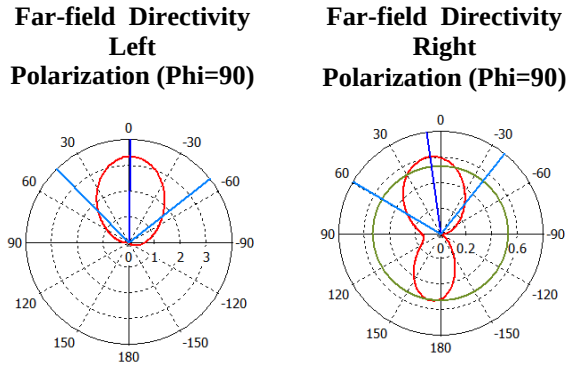

(b) YZ plane

Fig. 9. Simulated radiation patternsof the proposed antenna at 6.4 GHz.

Table 4. Comparison of the CP antenna with and without metasurface structure

Parameter	With metasurface structure	Without metasurface structure
BW (MHz)	676.3	650
Gain (dBic)	4.94	4.36
ARBW (MHz)	474.1	130
Radiation efficiency (%)	>81	>72

According to our proposed antenna's VSWR (Voltage Standing Wave Ratio) curve in Fig. 7, we can see that the calculated value is less than 2 throughout the operating band (6.436 – 7.138) GHz, so it is considered suitable for most antenna applications. The radiation efficiency is shown in Fig. 8, which is greater than 81% throughout the operating band. Fig. 9(a) and Fig. 9(b) depict the simulated radiation patterns at XZ and YZ plane respectively. The performance of our proposed metasurface based CP antenna is compared with the CP antenna without implementing metasurface structure in Table 4. From the table, we can conclude that the implementation of the metasurface structure to the CP antenna improves the antenna performance significantly.

Our proposed antenna is also compared with the other recently published work in Table 5 in terms of its size, BW, ARBW and gain. The comparison shows that the proposed antenna achieves a better gain and wider bandwidth than the other state-of-arts.

Table 5. Performance comparison table

Ref.	f_{ZOR} (GHz)	Overall antenna size (mm)	BW (%)	ARBW (%)	Gain (dBic)
[11]	5.5	20×20×2.4	11.55	2.54	4.36
[24]	5.2	60×60×2	4	4	8.6
[25]	5.8	32.3×32.3×1.5	3.97	--	0.92
[26]	2.64	25×25×1.6	7.6	--	3.17
[27]	2.08	70×78.5×0.8	22	--	1.4
[28]	2.4	66×66×258	10.10	6.06	4.6
This work	6.4	20×20×2.4	9.95	7.32	4.94

4. CONCLUSION

An antenna with wide bandwidth has been proposed by implementing metasurface structure. Employment of the metasurface structure improves antenna gain as well. The simulated results show an impedance bandwidth of 676.3 MHz with a gain of 4.94 dBic at a centre frequency of 6.796 GHz. The proposed low-profile and compact antenna can be easily incorporated to the other microwave devices that working at the same frequency band for particular application. The antenna's operating frequency is 6.458 GHz to 7.1343 GHz, which is applicable for satellite communication, Wi-Fi devices, weather radar systems, wireless applications and surveillance.

5. REFERENCE

[1] W. J. Yang, Y. M. Pan, and S. Y. Zheng, "A Low-Profile Wideband Circularly Polarized Crossed-Dipole Antenna with Wide Axial-Ratio and Gain Beamwidths," *IEEE Trans. Antennas Propag.*, vol. 66, no. 7, pp. 3346–3353, 2018.

[2] H. H. Tran and I. Park, "A Dual-Wideband Circularly Polarized Antenna Using an Artificial Magnetic Conductor," *IEEE Antennas Wirel. Propag. Lett.*, vol. 15, no. c, pp. 950–953, 2016.

[3] W. Yang, Y. Pan, S. Zheng, and P. Hu, "A Low-Profile Wideband Circularly Polarized Crossed-Dipole Antenna," *IEEE Antennas Wirel. Propag. Lett.*, vol. 16, no. c, pp. 2126–2129, 2017.

[4] L. Zhang *et al.*, "Single-feed ultra-wideband circularly polarized antenna with enhanced front-to-back ratio," *IEEE Trans. Antennas Propag.*, vol. 64, no. 1, pp. 355–360, 2016.

[5] B. Park and J. Lee, "Omnidirectional Circularly Polarized Antenna Utilizing Zeroth-Order Resonance of Epsilon Negative Transmission Line," vol. 59, no. 7, pp. 2717–2721, 2011.

[6] R. L. Transmission-line, C. Zhou, G. Wang, Y. Wang, B. Zong, and J. Ma, "CPW-Fed Dual-Band Linearly and Circularly Polarized Antenna

Employing Novel Composite," vol. 12, pp. 1073–1076, 2013.

[7] S. Ko, B. Park, and J. Lee, "Dual-Band Circularly Polarized Patch Antenna," vol. 12, pp. 1165–1168, 2013.

[8] N. I. Zheludev and Y. S. Kivshar, "From metamaterials to metadevices," *Nat. Mater.*, vol. 11, no. 11, pp. 917–924, 2012.

[9] V. Angoth, A. Singh, and M. S. Shanka, "A Novel Refractive Technique for Achieving Macroscopic Invisibility of Visual Light," vol. 1, no. 1, pp. 5–8, 2013.

[10] T. Cai, G. Wang, X. Zhang, and J. Shi, "Low-profile Compact Circularly-Polarized Antenna Based on Fractal Metasurface and Fractal Resonator," *IEEE Antennas and Wireless Propagation Letters*, vol. 1225, no. 3, pp. 1-4, 2015.

[11] M. Ameen and R. K. Chaudhary, "Metamaterial-based circularly polarised antenna employing ENG-TL with enhanced bandwidth for WLAN applications," *Electronics Letters*, vol.54, no.20, pp. 1152-1154, April 2018.

[12] E. Starodubtsev, "Features of reflection of electromagnetic waves from nanometric perforated multilayers including epsilon-near-zero metamaterials," *EPJ Appl. Metamaterials*, vol. 6, p. 22, 2019.

[13] T. Yamaguchi, T. Ishiyama, T. Ueda, and T. Itoh, "Enhancement of inductance along metallic mesh wires in three-dimensional quasi-isotropic metamaterials using high- ε dielectric particles for impedance-matching with free space," *EPJ Appl. Metamaterials*, vol. 6, p. 21, 2019.

[14] A. Li, S. Singh, and D. Sievenpiper, "Metasurfaces and their applications," *Nanophotonics*, vol. 7, no. 6, pp. 989–1011, 2018.

[15] D. J. Park, S. J. Park, I. Park, and Y. H. Ahn, "Dielectric substrate effect on the metamaterial resonances in terahertz frequency range," *Curr. Appl. Phys.*, vol. 14, no. 4, pp. 570–574, 2014.

[16] C. L. Holloway, E. F. Kuester, J. A. Gordon, J. O'Hara, J. Booth, and D. R. Smith, "An overview of the theory and applications of metasurfaces: The two-dimensional equivalents of metamaterials," *IEEE Antennas Propag. Mag.*, vol. 54, no. 2, pp. 10–35, 2012.

[17] Q.Chen and H. Zhang, "Dual-Patch Polarization Conversion Metasurface-Based Wideband Circular Polarization Slot Antenna," *IEEE Access*, vol. 6, no. c, pp. 74772–74777, 2018.

[18] B. Ratni, E. Bochkova, G. P. Piau, A. De Lustrac, A. Lupu, and S. N. Burokur, "Design and engineering of metasurfaces for high-directivity antenna and sensing applications," *EPJ Appl. Metamaterials*, vol. 3,pp. 1-4, March2016.

[19] C. Arora, S. S. Pattnaik, and R. N. Baral, "Bandwidth enhancement of microstrip patch antenna array using spiral split ring resonator," *Adv. Intell. Syst. Comput.*, vol. 672, no. 18, pp. 435–441, 2018.

[20] R. K. Saraswat and M. Kumar, "Implementation of Vertex-Fed Multiband Antenna for Wireless Applications with Frequency Band Reconfigurability Characteristics," *Wirel. Pers. Commun.*, pp 12, 2018.

[21] Wojciech Jan Krzysztofik and Thanh Nghia Cao,"Metamaterials in Application to Improve Antenna Parameters,"*Metamaterials and Metasurfaces*, Josep Canet-Ferrer,pp. 67, November 5, 2018.

[22] I. Park, "Application of metasurfaces in the design of performance-enhanced low-profile antennas," *EPJ Appl. Metamaterials*, vol. 5, 2018.

[23] C. Zhang, P. Gao, M. Sun, and T. Mu, "Analysis of the resonant frequency of the octagonal split resonant rings with metal wires," *Appl. Opt.*, vol. 49, no. 29, pp. 5638–5644, 2010.

[24] W. Han, F. Yang, R. Long, L. Zhou, and F. Yan, "Bandwidth enhancement for single-feed circularly polarised microstrip antenna with epsilon-negative transmission line-based annular ring," *Electron. Lett.*, vol. 51, no. 19, pp. 1475–1476, 2015.

[25] Q. X. Chu, M. Ye, and X. R. Li, "A Low-Profile Omnidirectional Circularly Polarized Antenna Using Planar Sector-Shaped Endfire Elements," *IEEE Trans. Antennas Propag.*, vol. 65, no. 5, pp. 2240–2247, 2017.

[26] R. K. Singh and A. Gupta, "CRLH Transmission Line Based Compact Metamaterial Inspired Antenna for Wi-MAX Applications," no. 1, pp. 1–4, 2020.

[27] A. Gupta and R. K. Chaudhary, "A Compact Planar Metamaterial Triple-Band Antenna with Complementary Closed-Ring Resonator," *Wirel. Pers. Commun.*, vol. 88, no. 2, pp. 203–210, 2016.

[28] X. Qing, J. Shi, and Z. N. Chen, "Metamaterial-based omnidirectional circularly polarized antenna array for 2.4-GHz WLAN applications," *2016 10th Eur. Conf. Antennas Propagation, EuCAP 2016*, pp. 3–5, 2016.